Transferable Models to Understand the Impact of Lockdown Measures on Local Air Quality

Johanna Einsiedler*, Yun Cheng‡, Franz Papst†, Olga Saukh†
*Vienna University of Business Economics / CSH Vienna, Austria. johanna_einsiedler@gmx.at
†Graz University of Technology / CSH Vienna, Austria. {papst, saukh}@tugraz.at
‡Computer Engineering and Networks Lab, ETH Zurich, Switzerland. chengyu@ethz.ch

***Abstract*—The COVID-19 related lockdown measures offer a unique opportunity to understand how changes in economic activity and traffic affect ambient air quality, and how much pollution reduction can the society offer through digitalization and mobility-limiting policies. In this work, we estimate pollution reduction over the lockdown period by using the measurements from ground air pollution monitoring networks, training *long-term* prediction models and comparing their predictions to measured values over the lockdown month. We show that our models achieve state-of-the-art performance and evaluate up to -29.4 %, -28.1 %, and -52.8 %, change in NO2 in Eastern Switzerland, Beijing and Wuhan respectively. Our reduction estimates take local weather into account. What can we learn from pollution emissions during lockdown? The lockdown period was too short to train meaningful models from scratch. We therefore use transfer learning to update only mobility-dependent variables. We show that the obtained models are suitable for the analysis of the post-lockdown periods and capable of estimating the future air pollution reduction potential.**

I. Introduction

Air quality is of vital importance to human health as has been shown in numerous medical studies [1], [2], [3]. Furthermore, air pollution leads to enormous economic losses [4] and its reduction is particularly important in overpopulated urban areas. In the context of the current pandemic, recent studies show that long-term exposure to air pollutants such as PM2.5 (particulate matter of diameter less than 2.5 micrometers) and NO2 (nitrogen dioxide) increases human susceptibility to SARS-CoV-2 [5], [3] and contributes to higher fatality rates [6], [7]. Lockdown measures of varying duration and strictness in response to COVID-19 have shown to be effective to slow down the virus spread in many countries. At the same time, reduced mobility, working from home, accelerated digitalization and e-commerce made researchers wonder about the pollution reduction potential also in the context of global warming and while preserving the basic operations of cities and counties.

Lockdowns provide a unique and valuable opportunity to analyze the air pollution reduction patterns. Fig. 1 presents a comparison of measured air pollution in Wuhan, China over the same period of time in 2019 and 2020. Due to significantly reduced human activities, such as traffic, the concentrations of NO2 drop to low and stable levels during the lockdown compared to the same period in 2019. Although numerous studies estimate pollution reduction during lockdown in various countries [8], [9], [10], [5], the results mostly represent

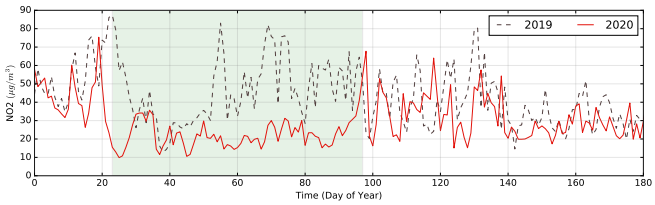

Fig. 1: NO2 measured in 2019 and 2020 from Jan 1 to June 30 in Wuhan, China. Green zones show the lockdown period from Jan 23 to Apr 27, 2020.

aggregated differences to various baselines. A detailed analysis of the lockdowns are difficult due to their short duration and, thus, scarceness of the representative data. This paper proposes a modelling framework that enables such analysis, and gives arguments for its usefulness in broader contexts.

Today, air pollution is measured by networks of governmental stations, satellite images [11], IoT devices [12], passive samplers, crowdsourcing campaigns, etc. Real-time air quality information from public [13] and private [14] stations can often be found online in many areas around the world. Numerous models were developed aiming at predicting short-term [15] and long-term pollution exposure [16] ranging from country-scale [17] to city-scale [18], [19], [20]. Although there is a large body of literature investigating the relationship between industry, traffic and air pollution, it is still not well understood how *changes* in economic activity and traffic affect ambient air quality [21].

Challenges. COVID-19 related lockdowns offer a chance to build more knowledge in this area. However, there are numerous challenges to be solved. (1) Recent studies investigating the impact of the lockdown measures on air pollution are not correcting for the influence of weather conditions on air pollution, which can considerably distort the obtained estimates. (2) Strict initial lockdown measures took place only for a few weeks in countries around the world, which complicates learning a reasonable model for the lockdown period. Later lockdowns incorporated a different set of measures and thus can not be used to enhance the training data. Solving the first challenge helps to accurately compute the local pollution reductions over the lockdown period and understand their spatio-temporal variability. Solving the second challenge enables learning from the lockdown experience by computing different

scenarios, such as estimating the air pollution reduction due to a partial back-to-normal regime or predicting pollution patterns if the lockdown would have happened during a different season or if its duration would have been extended.

Contributions and road-map. In this paper, we solve the above challenges by building *the first long-term predictive models for the lockdown period* (*LD* models). We use the following pipeline to achieve the goal: (1) Using historical data of several years before the lockdown, we train long-term pre-lockdown (*pre-LD*) models using Generalized Additive Models (GAMs) and show that they achieve comparable accuracy to the long-term models described in the literature. The *pre-LD* models are used to predict air pollution for the lockdown period while taking weather conditions into account. (2) The predictions are then compared to the actually measured values over the same period. (3) As next, we train weather-aware *LD* models using scarce lockdown data. We fix environmental dependencies in the models and use transfer learning to compute a new fit solely for the daytime dependent parameters. By cross-validation, we show that scarce data over 4 weeks of lockdown are sufficient to train accurate *LD* models for NO2. We use both model classes to analyze the post-lockdown data. Our approach is evaluated on three data sets from China and Switzerland. A more detailed analysis, also for Wuhan and Lower Austria, is available in the technical report [22]. The code is publicly shared on GitHub[1]. Sec. II summarizes a rapidly growing body of related works on modelling air pollution exposure.

II. Related Work

Big data has a huge impact on modelling environmental processes [23]. In contrast to short-term predictive models which increasingly leverage deep learning methods, long-term environmental predictions are largely rooted in scientific theory, which is one of the key reasons for their predictive power [24]. Below we summarize related works on data-driven air pollution models and discuss the challenges we face when applying these to estimating pollution reductions due to COVID-19 lockdown measures.

Long-term air pollution models. Classical dispersion models [25] are widely used for air quality mid-term and long-term predictions. These models identify the root cause of air pollution from chemical, emission, climatological factors and combinations thereof. A fitted model can then be used to understand the impact of each of these factors in isolation. Over the past years, GAMs have been frequently used to model air pollution and analyze the learned dependencies [18], [26], [27], [28], *e.g.*, to estimate the impact of weather on NO2, PM and O3 for Melbourne [27]. Belusic *et al.* [28] analyze the impact of meteorological variables numerically in their models and explain 45% of variance in CO, 14% in SO2, 25% in NO2 and 24% in PM10. In this work, we apply the model selection procedure in [16] to find the best hyperparameters and leverage the additive property of GAMs to tackle data scarcity issue when training *LD* models.

Short-term air pollution models. Recent models for short-term air quality prediction range from a few hours to a few days ahead and mainly rely on deep learning methods. FFA [29] forecasts air quality from meteorological and weather inputs. DeepAir [30] simultaneously considers individual and holistic influences. To further improve the model capacity, GeoMAN [31] used a three stage attention model learned from local features, global features and temporal geo-sensory time series. Lin *et al.* [32] represent the spatial correlations in a graph with automatically selected important geographic features that affect PM2.5 concentrations, and use these features to compute the adjacency graph for the model. To conquer the challenge of sample scarcity, Chen *et al.* [33] proposed a multi-task approach to learn the representations from the relevant spatial and sequential data, as well as to build the correlation between air quality and these representations. Zhang *et al.* [15] found that local fine-grained weather data is helpful to predict air quality. These deep learning approaches focus on very short time horizons significantly shorter than the duration of COVID-19 related lockdowns. For this reason, this paper relies on GAMs as our basic modelling approach.

Transferable models. Transfer learning [34] promises to light-retrain a model in order to adapt the parameters to a changed setting and requires little data. Pollution models are usually not spatially transferable, *e.g.*, across cities and countries, because the learned dependencies are location-specific and policies may vary substantially across distant areas. Also temporal transferability of learned dependencies is difficult since land-use, environmental characteristics and policies may change over time. Thus, a few pollution model transfer examples from the literature extensively leverage prior expert knowledge or make strong assumptions about the structure of the source and the target domains such as shared similarities and other transferable structures [35], [36]. This paper makes use of an abrupt change of economic activity within the lockdown period, whereas land-use, environmental characteristics and policies remained essentially the same. This makes temporal model transfer possible and feasible.

Impact of COVID-19 on air quality. Lockdown measures in response to COVID-19 pandemic offer a unique opportunity to improve prediction of policy impacts reinforcing work-from-home and changing to low-emission mobility vehicles. The study in [37] assessed NO2 reduction based on satellite imagery by NASA and ESA in multiple COVID-19 epicenters. A similar assessment of other areas is provided in [11]. The relationship between air pollution and lockdown measured was studied in [9] using satellite data and ground sensors. The weather dependency is modelled as a simple linear function. A recent report [38] estimates NO2 reduction for major European cities during spring lockdowns when compared to previous years. Building a good predictive model for the lockdown period is challenging due to a short lockdown duration of only several weeks in most countries. In contrast to all previous efforts, we are one of a few to provide a weather and season-

[1] https://github.com/johanna-einsiedler/covid-19-air-pollution

Country	Class	Local situation	# stations
East Switzerland	No Traffic	Located offside the road	1
	Low Traffic	≤30,000 VPD	3
	High Traffic	>30,000 VPD	1
China	Urban	Urban Beijing, parks	12
	Rural	Countryside, parks	11
	Suburban	Polluted transfer zones	7
	Road	Urban, high traffic	5

TABLE I: Classification of stations in Switzerland by #vehicles per day (VPD) and in China by location type for NO2.

compensated estimates of pollution reduction over the lockdowns in 2020[2], and we are the first to use transfer learning to train a long-term model for the COVID-19 lockdown period.

III. Data Sets

This section describes the data sets we use to train and test the *pre-LD* and *LD* models for China and Switzerland. We also shortly describe the progress and the duration of the lockdown measures. Note that the investigated countries implemented very different air pollution reduction policies over the years. Also the severity of the lockdown measures varied considerably throughout 2020. Both facts highlight robustness of the modelling approach presented in the paper.

Eastern Switzerland. Air quality data and weather data for Eastern Switzerland are published by Ostluft[3]. The stations measure main air pollutants along with meteorological data. Stations are spread across the area, although bigger cities including Zurich and St. Gallen have more than one station at representative locations. We use the available 5 stations that provide data on NO2 and weather conditions including wind direction over the period from Jan 1, 2016 to Feb 5, 2021. The initial lockdown in Switzerland took place between Mar 16 and Apr 27, 2020 [39] and was much stricter than later measures. According to the traffic conditions, we classify the stations into three groups[4]: *No Traffic*, *Low Traffic* and *High Traffic*. The details are summarized in Table I.

Beijing and Wuhan. We collect air quality data[5],from 35 stations in Beijing and 10 stations in Wuhan from Jan 1, 2016 to Feb 5, 2021. Our scripts also fetch meteorological data[6] for the same locations. The initial lockdown periods in Beijing and in Wuhan were between Jan 23 and Apr 8, 2020. Further lockdowns were considerably lighter or affected only local areas. Air quality stations in Beijing have been categorized into four classes by the local authorities as shown in Table I: *Road*, *Rural*, *Suburban* and *Urban*.

In all considered areas, the available data has hourly time resolution. We use daily aggregates to train and validate our models. Note that the lockdown severity in Wuhan was the highest and in Switzerland the lowest.

[2]A study based on Random Forest models reporting similar results for Switzerland can be found here: https://bit.ly/2RX2Oml visited 2020-10-26.

[3]https://www.ostluft.ch/ visited 2021-01-25

[4]https://www.ostluft.ch/index.php?id=19 visited 2021-01-25

[5]https://quotsoft.net/air/ visited 2020-10-12

[6]https://darksky.net/ visited 2021-02-05

IV. Long-Term Predictive Models

This section describes the process of training a *pre-LD* model to predict air pollution if no lockdown would have happened. We rely on a model-based approach, since the prediction time horizon should cover the whole lockdown period of several weeks and thus the trained models should have sufficient predictive power for long-term predictions. We adopt GAMs that have successfully been used to model air pollution in the past [18]. In addition, we leverage optimizations [16], [40] and statistical tests to ensure model robustness and high performance as described below. As air pollution is highly sensitive to the local environment, it is necessary to fit a separate model for each station.

A. Generalized Additive Models (GAMs)

In GAMs, the impact of the predictive variables is captured through non-parametric smooth functions. These are summed up and related to the response variable via a link function:

$$g(E(Y)) = s_1(x_1) + s_2(x_2) + ... + s_p(x_p), \quad (1)$$

where $E(Y)$ is the expected value of the dependent variable Y, $g(\cdot)$ is a link function between its argument and the expected value to the predictor variables $x_1, ..., x_p$, and $s_1(\cdot), ..., s_p(\cdot)$ denote non-parametric smooth functions. The statistical distribution of the concentration of air pollutants, similarly to many other environmental parameters, closely follows a log-normal distribution [41]. A logarithmic link function $g(\cdot)$ has been chosen similarly to [18].

B. Explanatory Variables

The explanatory variables comprise meteorological parameters: wind speed (WS), wind direction (WD), precipitation (P), temperature (T), dew point (DP) and relative humidity (RH). To ensure an accurate feature representation of the wind direction, the polar coordinates are transformed into cartesian coordinates: $\text{WD}_x = \sin\left(\frac{\text{WD}}{360} \cdot 2\pi\right), \text{WD}_y = \cos\left(\frac{\text{WD}}{360} \cdot 2\pi\right)$. Furthermore, an additional variable is created by applying principal component analysis (PCA) on precipitation, humidity, dew point and temperature. PCA is a dimensionality reduction method to reduce the mutual correlations between included variables. The first component is added to the set of explanatory variables as PCA. We augment the set of explanatory variables with their lagged versions for one, two and three days. Wind speed (WS) and PCA are augmented with their respective rolling averages over the previous weeks. In addition, a categorical variable for month (M) and a variable for day of the year (DY) is included to account for seasonal patterns.

C. Model Selection Algorithm

For the selection of the model covariates we use a forward elimination procedure. The algorithm closely follows the framework used in similar research designs [16], [40]. Two key indicators are used for the model selection: the Akaike Information Criterion (AIC) [42] and the Variance Inflation Factor (VIF) [43]. The AIC is an estimate of the in-sample

Variable name	Abbr.	Switzerland		Beijing		Wuhan	
		NO2	PM10	NO2	PM2.5	NO2	PM2.5
Wind speed	WS	4	5	32	32	5	-
Wind dir. X	WD_x	6	8	18	21	8	10
Wind dir. Y	WD_y	3	4	7	7	11	11
Precipitation	P	-	-	-	-	-	-
Temperature	T	2	5	1	-	-	-
Rel. humidity	RH	2	3	21	9	11	9
Month	M	-	-	-	-	-	1
Day of year	DY	2	-	24	3	4	8
Dew point	DP	0	-	7	1	1	-
PCA	PCA	7	-	26	21	4	9
Weekday	D	1	2	-	2	1	-

TABLE II: # stations where the corresponding explanatory variable was chosen by the model selection algorithm.

prediction error that is commonly used to compare the quality of different statistical models for a given data set [44]. The aim of the indicator is to regularize the model by balancing the goodness-of-fit against model complexity and thereby avoiding both underfitting and overfitting. It is calculated as AIC = $2k - \ln(l)$, where k is the number of model parameters, and l denotes the maximum value of the model likelihood.

The VIF measures the degree of collinearity between independent variables. Collinearity inflates the variance of regression parameters and may lead to wrong identification of the relevant predictors [45]. It is calculated as VIF = $1/(1 - R_i^2)$, where R_i^2 is the coefficient of determination of the regression of the i-th variable over all other explanatory variables.

Model selection algorithm. The algorithm closely follows [16] and executes as follows: (1) For each explanatory variable we fit a GAM model comprising just this single variable. The model with the lowest AIC is selected. (2) We iteratively search for the next best variable to be added to the model. Variables with $VIF > 2.5$ are filtered out. Among the constructed candidate models, the one with the lowest AIC is chosen. The threshold of 2.5 corresponds to the coefficient of determination $R^2 = 0.6$. This conservative setting was deemed appropriate taking into account collinearity of weather variables. Scientific papers dealing with weather data often adopt the threshold of 2.5 [16], whereas higher cut-off values, *e.g.*, 4, 5 and 10, are also found in the literature [46], [40]. Step (2) is repeated until the addition of any further explanatory variable leads to an increased AIC.

The results of the model selection algorithm for all stations in China and Switzerland are shown in Table II. The value in each cell represents the frequency of the corresponding explanatory variable being selected by the algorithm into a GAM model. Ultimately, the Weekday variable (D) was explicitly added to all models to take into account traffic-induced weekly pollution periodicity. This technique has been used in a similar research design to analyse long-term air pollution trends [16]. We adopt this technique in order to later be able to learn the *LD* model from the *pre-LD* model using transfer learning.

D. Model Validation

We assess the quality of the trained *pre-LD* models using cross-validation. The root-mean squared error (RMSE) is used to assess prediction quality. The results for NO2 for Switzerland and Beijing are exemplified in Fig. 2. We train models for different stations on 3, 6, 9, 12, 18 and 24 months of data prior to a chosen date and test these on the data for the subsequent month. The chosen cut-off date is the start of each month in the year 2019. We observe that up to two years of data is necessary to train the *pre-LD* GAM models of acceptable quality. Further evaluation is based on the *pre-LD* models trained on two years of data preceding the lockdown in each region.

Eastern Switzerland. In cross-validation, the models have an average RMSE of 7.2 for NO2 and 5.0 for PM10. Barmpadimos et al. [16] use GAMs fitted on detailed weather data to analyse PM10 trends in Switzerland. Their models fitted on 16 years of data reach a RMSE between 2.2 and 3.2 for PM10, see Table III. We conclude that the quality of the obtained GAM models trained on less data is only marginally worse compared to the published results.

Beijing. For the stations in Beijing the average RMSE for PM2.5 in cross validation is 29.4. Zhang et. al. [15] compare different models for *short-term* (between 6 h and 24 h) PM2.5 predictions in Beijing over 2016-2018. The RMSE of these short-term models ranges between 26.9 and 44.1. Our long-term models have only slightly worse performance compared to the state-of-the-art short-term deep learning models. In contrast to these short-term models, our GAMs need significantly more (two years compared to a few days) training data to achieve acceptable accuracy. We note that historical weather data is often publicly available, which makes model training on large historical data sets possible.

In the next section, we use the trained *pre-LD* models to estimate pollution reduction due to the COVID-19 lockdown measures. We mainly showcase the results for NO2. Further analysis for PM10 and PM2.5 data is available in our technical report [22].

V. Impact of COVID19 on Air Pollution

The most common approach to estimate the impact of COVID-19 intervention measures on air pollution is based on the comparison of the measured values over the lockdown period in 2020 to the same time interval in 2019. However, air pollution is known to depend on weather conditions, seasonal as well as policy updates that prohibit an accurate estimation of pollution reductions due to lockdowns. In this section we estimate pollution reduction while taking weather-related parameters into account.

Local weather highly impacts the daily change of air pollution. In Fig. 3, we compare weather conditions during the lockdown period in 2020 and during the same period in 2019. We observe that in Switzerland, the lockdown weather was warmer, dryer, and less windy than in 2019. Similar observations apply to Beijing and Wuhan. In addition, we notice a change in the wind direction, which is a significant

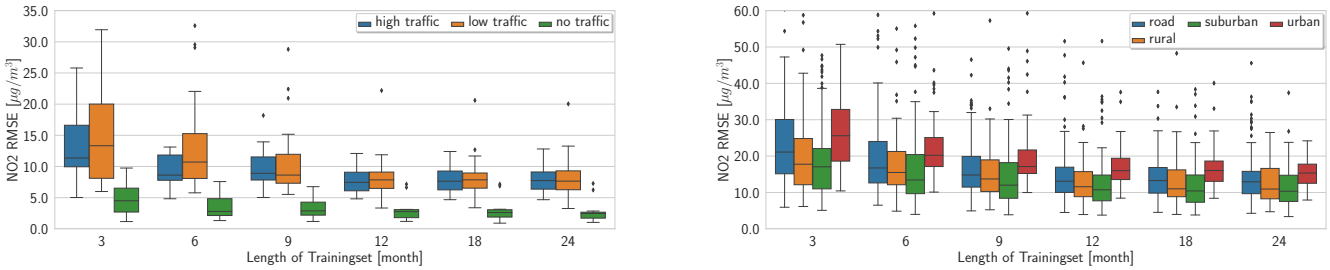

(a) Switzerland NO2

(b) Beijing NO2

Fig. 2: *pre-LD* model performance in cross-validation using different lengths of the train data.

Model	Measure	Switzerland NO2 $\mu g/m^3$	Switzerland PM10 $\mu g/m^3$	Beijing NO2 $\mu g/m^3$	Beijing PM2.5 $\mu g/m^3$	Wuhan NO2 $\mu g/m^3$	Wuhan PM2.5 $\mu g/m^3$
pre-LD	RMSE	7.16	4.99	13.38	29.41	14.61	22.37
	R^2	0.69	0.54	0.60	0.55	0.64	0.66
LD	RMSE	7.03	-	13.08	-	12.26	-

(a) *pre-LD* and *LD* model performance in cross-validation.

Measure	Switzerland Barmpadimos *et al.* [16] PM10 $\mu g/m^3$	Beijing Zhang *et al.* [15] PM2.5 [1-6h] $\mu g/m^3$	Beijing Zhang *et al.* [15] PM2.5 [19-24h] $\mu g/m^3$
RMSE	2.60	17.35 – 25.81	26.88 – 44.08
R^2	0.62	-	-

(b) Comparison to related works.

TABLE III: *pre-LD* and *LD* model performance in cross-validation, comparison to related works.

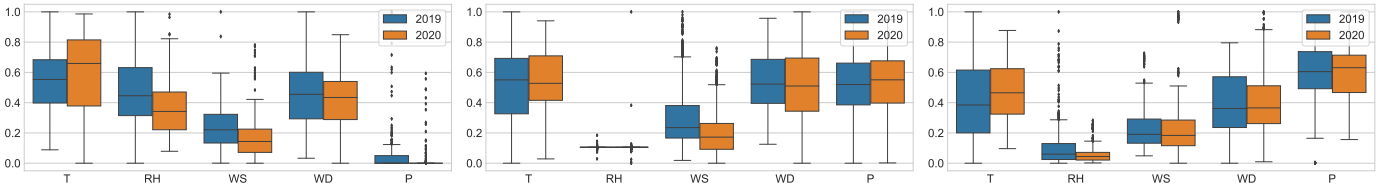

(a) Switzerland

(b) Beijing

(c) Wuhan

Fig. 3: Weather comparison for the lockdown periods in 2020 to the same period in 2019 in Switzerland, Beijing and Wuhan.

pollution predictor in these regions due to a strong pollution transfer phenomenon [15]. The significant role of wind in the Beijing and Wuhan models is also reflected in Table II by a high number of the *pre-LD* GAM models where WS, WD_x and WD_y were chosen as important explanatory variables by the model selection algorithm.

To estimate pollution reduction during lockdowns, we leverage the *pre-LD* models trained on the pre-LD data as outlined in Sec. IV, and use these to predict air pollution concentrations over the lockdown periods. We then compute the difference between the predicted and the actually measured values to estimate the impact of the lockdown measures in each region. Overall, the estimated NO2 change over the LD period compared to the same time period in 2019 in Switzerland evaluates to -29.4 %. For Beijing and Wuhan we estimate changes of -28.1 % and -52.8 %, respectively.

Eastern Switzerland. Since NO2 is highly impacted by traffic, we put the obtained NO2 reduction estimates in the context of traffic reduction reported by Apple based on the observed change in usage of its services. The Apple Mobility Trends Report [47] publishes aggregated estimates of the changed driving behavior of their users based on the navigation requests. The data suggests an average reduction of driving activity in Switzerland of 40.4 % compared to the baseline of Jan 13, 2020. This traffic drop translated into a reduction of NO2 between 78.4 % and 35.5 % for Low Traffic and High Traffic stations respectively as predicted with our models, when using the same baseline. Fig. 4 compares the output of the *pre-LD* models to the observed values in 2019 and 2020 for these classes. For the station located off the road, we find an increase of 15.1 %. In this case, the average NO2 is very low and its positive change can be regarded as marginal and likely attributed to weather phenomena not captured by our explanatory variables. A similar increase of 27.4 % was reported by [8] for another rural station in Switzerland.

Beijing and Wuhan. We estimate an average NO2 reduction of -33.3%, and -64.1%, for Beijing and Wuhan for the same period as reported in [11], respectively. The detailed comparison for the traffic-based area breakdown is shown in Table IV. We compare our weather-aware predictions to the published results [11] obtained based on the analysis of the satellite images over the lockdown period (see TROPOMI [11] and OMI [11] in Table IV). Our NO2 reduction estimates fall within the confidence intervals of the satellite imagery based predictions. Sample predictions for the whole lockdown period of Jan 23 to Apr 9, 2020 for urban and rural stations in

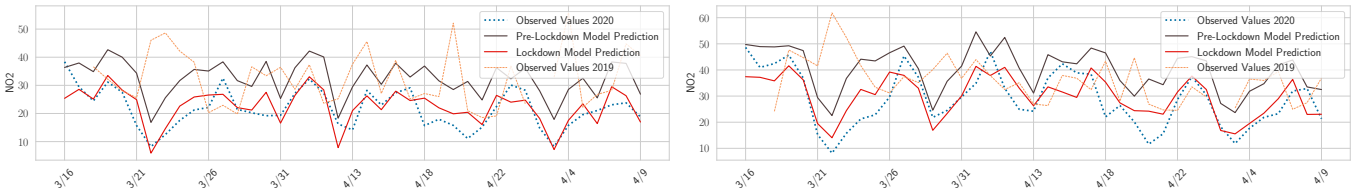

Fig. 4: Sample predictions for NO2 for high (left) and low (right) traffic in Eastern Switzerland.

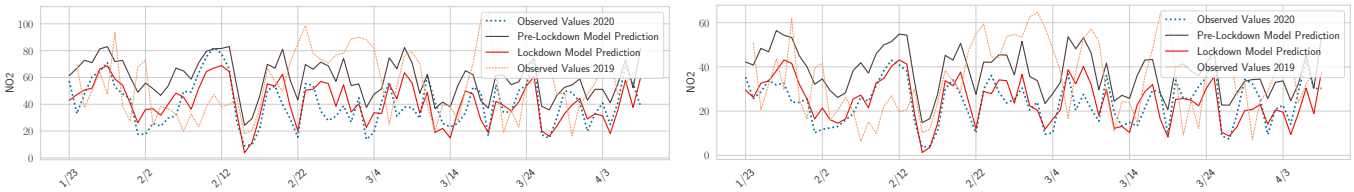

Fig. 5: Sample predictions for NO2 for road (left) and rural (right) areas in Beijing, China.

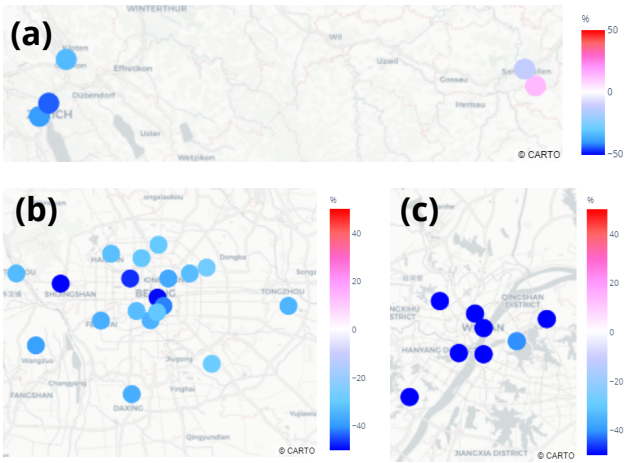

Fig. 6: Spatial distribution of NO2 reduction for (a) Switzerland, (b) Beijing and (c) Wuhan. Red means increasing and blue means reduction in the plot.

Estimators	Beijing				Wuhan
	Urban %	Suburban %	Rural %	Road %	%
pre-LD	-33.3	-25.8	-37.4	-33.1	-64.1
TROPOMI [11]	-25±10	-25±10	-25±10	-25±10	-43±14
OMI [11]	-33±10	-33±10	-33±10	-33±10	-57±14

TABLE IV: Estimated NO2 reduction in Beijing and Wuhan compared to [11] as measured by satellite imagery.

Beijing are exemplified in Fig. 5. Measured NO2 values are significantly below *pre-LD* predictions.

We also provide a spatial distribution of the pollution reductions over the lockdown period across all stations in our data sets in Fig. 6. When comparing major cities under analysis (Wuhan and Beijing in China; St. Gallen and Zurich in Eastern Switzerland), we conclude that NO2 reductions were higher in cities with stricter enforced intervention measures.

VI. Learning Lockdown Models

The lockdown period gives us a bottom-line by how much humans in different regions, given their cultural and political differences, can reduce their activities in a fear of getting infected by a virus. Having a bottom-line is useful when evaluating future policy changes, sector restructuring due to technological advances, process optimizations, etc. In this section we describe the construction of the *LD* models by transfer learning and show the value of both models in the analysis of the post-lockdown period.

Transfer learning is a popular technique to apply the knowledge gained by solving a particular task to a related task [35]. Since the lockdown period was too short to fit a GAM model for this time period, we apply transfer learning to *pre-LD* models to derive models for the lockdown period. In this step we re-train the models on the scarce lockdown data to only fit the variables where we suspect the dependencies may have changed due to lockdown, *i.e.*, the day of the week (D). These variables serve as proxy for the traffic intensity. All weather dependencies in the *LD* model are considered to be the same as in the *pre-LD* model, which is confirmed by the domain experts. The knowledge gained with regards to the influence of the weather and seasonality on air pollution can be transferred to the lockdown period. Thus, there is no need to train the entire model from scratch.

A. Model Validation

Due to data scarcity over the lockdown period of only several weeks, we test the performance of the *LD* model by 14-fold cross-validation by choosing 3 successive days within 6 weeks of initial lockdown as test data. The remaining data from the lockdown period is used for training. This way, we get 14 estimates for the out of sample prediction RMSE. The summary of the average RMSE values for the lockdown model can be found in Table III. In Eastern Switzerland, the *LD* model closely matches the observed values. On average, the

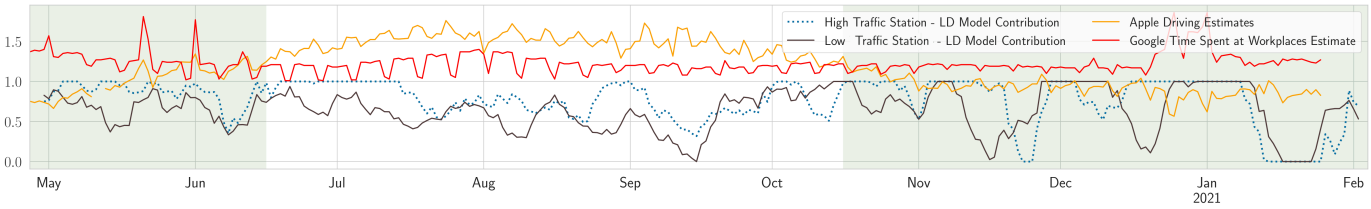

Fig. 7: Contribution of the *LD* model (α in (2)), estimates of changes in driving from the Apple Mobility Report [47] and estimated time spent at work places form the Google Community Mobility Report [48] compared to the report's respective baseline, for the time after the initial lockdown in Switzerland.

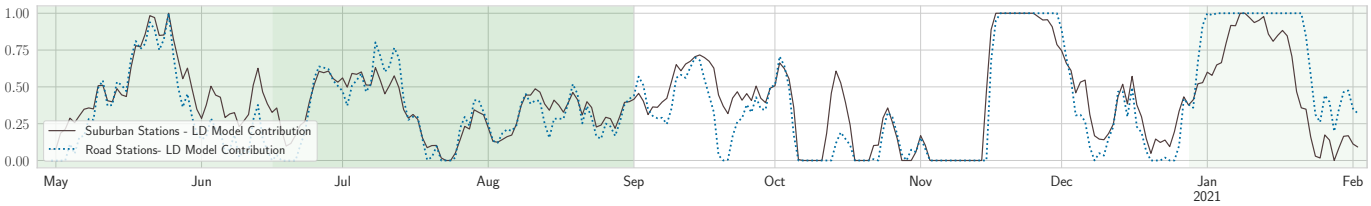

Fig. 8: Contribution of the *LD* model (α in (2)) for the time after the first lockdown in Beijing.

LD models have a RMSE of 7.03 whereas the *pre-LD* models have a RMSE of 7.16. This shows that the fine-tuned *LD* model reflects well the dependency between air pollution and explanatory variables for the short lockdown time period. For Beijing and Wuhan, we obtain a RMSE of 13.08 and 12.26 for the *LD* models for both cities respectively, compared to the RMSE of 13.38 and 14.61 of the *pre-LD* models. As next we show that the *LD* model can indeed be useful to analyze the impact of traffic reduction on air pollution.

B. Evaluation of the Post-Lockdown Period

We use both *pre-LD* and *LD* models to investigate the optimal mixture thereof capable of explaining the observed pollution values after the lockdown period. By doing so we aim to estimate to what extent have human mobility and the inherent traffic gone back to normal. To run this analysis, we minimize the absolute sum of differences between the true observations and the mixture of the *pre-LD* and *LD* model predictions:

$$\arg\min_{\alpha} \frac{1}{||T||} \sum_{t \in T} |\alpha \cdot m_t^{LD} + (1-\alpha) \cdot m_t^{pre\text{-}LD} - m_t|, \quad (2)$$

where m_t is the measured value at time $t \in T$, T is a post-lockdown period of length $||T||$ under consideration, m_t^{LD} and $m_t^{pre\text{-}LD}$ are the predictions obtained with *LD* and *pre-LD* models respectively. The dependent variable α shows the contribution of the *LD* model when explaining the post-lockdown pollution measurements. The results of this analysis for NO2 in China and Switzerland are summarized below and visualized in Fig. 7 and Fig. 8.

Eastern Switzerland. For Eastern Switzerland we analyze the data after the initial lockdown, which covers the time period between May 2020 and Feb 2021. The results in Fig. 7 show that the first months following the initial lockdown are close to the lockdown situation. Over summer the mobility gradually resumes back to ∼50 % normal again. However from Oct 2020 onwards, we can again observe a considerable traffic reduction due to mobility reducing measures put in place by the Swiss government in response to rising numbers of COVID cases [49]. From Dec 22, 2020 until the end of our dataset (Feb 5, 2021), Switzerland has been put under a lockdown again [50]. However, our model estimates a low reduction this time (between 18 % and 24 %) for the traffic exposed stations. The reason for this is only a limited decrease of traffic density: According to the mobility estimates by Apple [47], driving in Switzerland reduced by on average 40 % throughout the initial lockdown in spring 2020, whereas during the second ongoing lockdown, only a 15 % reduction has been observed.

Beijing. In Beijing the second lockdown was imposed between June 15, 2020 and Sept 1, 2020. For this time period we estimate a reduction in NO2 of 11 % for rural, 15 % for urban, 7 % for suburban and 23 % for road stations. These comparatively small reductions are to be expected as the second lockdown hasn't been nearly as strict as the first one. As shown in Fig. 8, only in October, NO2 values came back to their typical pre-COVID-19 levels in Beijing. Since Dec 29, 2020 a light, partial lockdown has been in place in some areas of Beijing [51] which resulted in a sudden return to a level of 100% lockdown model contribution, as highlighted in Fig. 8.

VII. Conclusion and Discussion

This paper proposes an approach to estimate the impact of the COVID-19 lockdown measures on local air quality as measured by ground measurement stations. Related works evaluate pollution reduction by comparing measured values to the same period in 2019 or by the analysis of satellite imagery. By contrast, our models learn a dependency between local air quality and weather augmented by the daytime-specific dynamics impacted by traffic. We train long-term *pre-LD* models using two years of historical data for the stations in Eastern

Switzerland and China and compare obtained predictions to measured values over the lockdown. Our analysis and findings match recent literature and show a significant decrease in NO2 in all areas.

Due to a short lockdown duration it is impossible to learn a meaningful model for the lockdown period from scratch. We use transfer learning to re-train only a subset of explanatory variables on the scarce lockdown data. The resulting *LD* models provide a bottom-line for the pollution reduction in various areas due to lockdown interventions. The model matches the quality of the state-of-art air pollution models and can be used in the analysis of the post-lockdown period.

REFERENCES

[1] D. Cory-Slechta, M. Sobolewski, E. Marvin, and *et al.*, "The impact of inhaled ambient ultrafine particulate matter on developing brain," *Toxicologic Pathology*, vol. 47, no. 8, pp. 976–992, 2019.

[2] R. Burnett, H. Chen, and *et al.*, "Global estimates of mortality associated with long-term exposure to outdoor fine particulate matter," *Nat. Academy of Sciences*, vol. 115, no. 38, pp. 9592–9597, 2018.

[3] J. Lelieveld, A. Pozzer, U. Pöschl, M. Fnais, A. Haines, and T. Münzel, "Loss of life expectancy from air pollution compared to other risk factors: a worldwide perspective," *Cardiovascular Research*, 2020.

[4] Dechezlepr$_f$ N. Rivers, and B. Stadler, "The economic cost of air pollution: Evidence from europe," Organisation for Economic Co-operation and Development, Working Paper 1584, 2019.

[5] Y. Han, J. Lam, V. Li, and *et al.*, "The effects of outdoor air pollution concentrations and lockdowns on covid-19 infections in wuhan and other provincial capitals in china," 2020, preprints.

[6] Y. Ogen, "Assessing NO2 levels as a contributing factor to COVID-19 fatality," *Science of The Total Environment*, vol. 726, p. 138605, 2020.

[7] X. Wu, R. Nethery, and *et al.*, "Exposure to air pollution and COVID-19 mortality in the united states," *medRxiv*, 2020.

[8] S. Grange, C. Hüglin, and L. Emmenegger, "Influence of COVID-19 lockdowns on Switzerland's air quality," 2020.

[9] Z. Venter, K. Aunan, S. Chowdhury, and J. Lelieveld, "Covid-19 lockdowns cause global air pollution declines with implications for public health risk," *medRxiv*, 2020.

[10] "Impact of COVID-19 led lockdown on air pollution levels in Bengaluru," Jun. 2020.

[11] M. Bauwens, S. Compernolle, and *et al.*, "Impact of coronavirus outbreak on NO2 pollution assessed using TROPOMI and OMI observations," *Geophysical Research Letters*, vol. 47, no. 11, Jun. 2020.

[12] O. Saukh, D. Hasenfratz, C. Walser, and L. Thiele, "On rendezvous in mobile sensing networks," in *RealWSN*, 2013, pp. 29–42.

[13] OSTLUFT, "Standortdatenblätter 2019." [Online]. Available: https://www.ostluft.ch/index.php?id=223

[14] D. Hasenfratz, O. Saukh, and *et al.*, "Participatory air pollution monitoring using smartphones," in *MobileSensing*, 2012, pp. 1–5.

[15] Y. Zhang, Q. Lv, and *et al.*, "Multi-group encoder-decoder networks to fuse heterogeneous data for next-day air quality prediction," in *Int. Joint Conf. on Artificial Intelligence*. AAAI Press, 2019, pp. 4341–4347.

[16] I. Barmpadimos, C. Hueglin, and *et al.*, "Influence of meteorology on PM_{10} trends and variability in switzerland from 1991 to 2008," *Atm. Chemistry and Physics*, vol. 11, no. 4, pp. 1813–1835, 2011.

[17] K. Ricke, L. Drouet, K. Caldeira, and M. Tavoni, "Country-level social cost of carbon," *Nature Climate Change*, vol. 8 (10), pp. 895–900, 2018.

[18] D. Hasenfratz, O. Saukh, C. Walser, and *et al.*, "Deriving high-resolution urban air pollution maps using mobile sensor nodes," *Pervasive and Mobile Computing*, vol. 16, pp. 268–285, 2015.

[19] M. Müller, D. Hasenfratz, O. Saukh, M. Fierz, and C. Hueglin, "Statistical modelling of particle number concentration in Zurich at high spatio-temporal resolution utilizing data from a mobile sensor network," *J. of Atmospheric Environment*, vol. 126, pp. 171–181, 2016.

[20] D. Hasenfratz, O. Saukh, C. Walser, C. Hueglin, M. Fierz, and L. Thiele, "Pushing the spatio-temporal resolution limit of urban air pollution maps," in *PerCom*, 2014, pp. 69–77.

[21] K. Wang, H. Yin, and Y. Chen, "The effect of environmental regulation on air quality: A study of new ambient air quality standards in china," *Journal of Cleaner Production*, vol. 215, pp. 268–279, 2019.

[22] J. Einsiedler, Y. Cheng, F. Papst, and O. Saukh, "Technical report: Transferable models to understand the impact of lockdown measures on local air quality," 2020.

[23] W. Pietsch and J. Wernecke, "Berechenbarkeit der Welt? Philosophie und Wissenschaft im Zeitalter von Big Data," in *Springer VS, Wiesbaden (eds Pietsch, W., Wernecke, J. and Ott, M.)*, 2017, pp. 37–57.

[24] D. Rolnick, P. L. Donti, L. H. Kaack, and *et al.*, "Tackling climate change with machine learning," *CoRR*, vol. abs/1906.05433, 2019.

[25] Y. Zhang, M. Bocquet, V. Mallet, C. Seigneur, and A. Baklanov, "Real-time air quality forecasting, part i: History, techniques, and current status," *Atmospheric Environment*, vol. 60, pp. 632–655, 2012.

[26] P. Bertaccini, V. Dukic, and R. Ignaccolo, "Modeling the short-term effect of traffic and meteorology on air pollution in turin with generalized additive models," *Advances in Meteorology*, vol. 2012, p. 609328, 2012.

[27] J. Pearce, J. Beringera, and N. N. *et al.*, "Quantifying the influence of local meteorology on air quality generalised additive modelling," *Atmospheric Environment*, vol. 6, no. 45, pp. 1328–1336, 2011.

[28] A. Belusic, I. Bulić, and Z. Klaic, "Using a generalized additive model to quantify the influence of local meteorology on air quality in Zagreb," *Geofizika*, vol. 32, p. 47, 2015.

[29] Y. Zheng, X. Yi, M. Li, R. Li, and *et al.*, "Forecasting fine-grained air quality based on big data," in *SIGKDD*, 2015, pp. 2267–2276.

[30] X. Yi, J. Zhang, Z. Wang, T. Li, and Y. Zheng, "Deep distributed fusion network for air quality prediction," in *SIGKDD*, 2018, pp. 965–973.

[31] Y. Liang, S. Ke, J. Zhang, X. Yi, and Y. Zheng, "Geoman: Multi-level attention networks for geo-sensory time series prediction." in *IJCAI*, 2018, pp. 3428–3434.

[32] Y. Lin, N. Mago, Y. Gao, Y. Li, Y. Chiang, C. Shahabi, and J. Ambite, "Exploiting spatiotemporal patterns for accurate air quality forecasting using deep learning," in *SIGSPATIAL*, 2018, pp. 359–368.

[33] L. Chen, Y. Ding, D. Lyu, X. Liu, and H. Long, "Deep multi-task learning based urban air quality index modelling," *Proceedings of the ACM on Interactive, Mobile, Wearable and Ubiquitous Technologies*, vol. 3, no. 1, pp. 1–17, 2019.

[34] S. Pan and Q. Yang, "A survey on transfer learning," *IEEE Trans. on knowledge and data engineering*, vol. 22, no. 10, pp. 1345–1359, 2009.

[35] Y. Wei, Y. Zheng, and Q. Yang, "Transfer knowledge between cities," in *Proceedings of the 22nd ACM SIGKDD International Conference on Knowledge Discovery and Data Mining*, 2016, pp. 1905–1914.

[36] Y. Cheng and *et al.*, "MapTransfer: Urban air quality map generation for downscaled sensor deployments," in *IoTDI*, 2020, pp. 14–26.

[37] S. Muhammad, X. Long, and M. Salman, "COVID-19 pandemic and environmental pollution: A blessing in disguise?" *Science of The Total Environment*, vol. 728, p. 138820, 2020.

[38] H. Thieriot and L. Myllyvirta, *Air pollution returns to European capitals: Paris faces largest rebound.* Centre for research on Energy and Clean Air, 2020.

[39] S. Bundesrat, "Verordnung 2 über massnahmen zur bekämpfung des coronavirus (covid-19)," Mar. 2020.

[40] N. Carslaw, D. Carslaw, and K. Emmerson, "Modelling trends in oh radical concentrations using generalized additive models," *Atmospheric Chemistry and Physics*, pp. 2021–2033, Mar. 2009.

[41] E. Limpert, W. Stahel, and M. Abbt, "Log-normal Distributions Across the Sciences," *BioScience*, vol. 51, no. 5, pp. 341–352, 05 2001.

[42] H. Akaike, "A new look at the statistical model identification," *IEEE Trans. on Automatic Control*, vol. 19, no. 6, pp. 716–723, Dec. 1974.

[43] R. Freund, W. Wilson, and P. Sa, *Regression Analysis*. Elsevier, 2006.

[44] T. Hastie, R. Tibshirani, and J. Friedman, *The Elements of Statistical Learning*, 1st ed. Springer, 2001.

[45] C. Dormann, J. Elith, S. Bacher, and *et al.*, "Collinearity: a review of methods to deal with it and a simulation evaluating their performance," *Ecography*, no. 36, pp. 27–46, 2013.

[46] R. M. O'Brien, "A caution regarding rules of thumbfor variance inflation factors," *Quality & Quantity*, no. 41, pp. 673–690, 2007.

[47] Apple, "Mobility trends report," 2020. [Online]. Available: www.covid19.apple.com/mobility

[48] Google, "Community mobility reports," 2020. [Online]. Available: www.google.com/covid19/mobility/

[49] "BAG: Bund verstärkt massnahmen," https://bit.ly/3eQeXCq, 2021.

[50] Südkurier, "Schweiz geht in den lockdown," https://bit.ly/3htxxlM, 2021.

[51] Reuters, "China's capital locks down part of district in coronavirus fight," https://www.reuters.com/article/us-health-coronavirus-china-beijing-idUSKBN2930TL, 2021.